

COMPTEL OBSERVATIONS OF COSMIC GAMMA-RAY BURSTS

C. Winkler⁴, K. Bennett⁴, H. Bloemen², H.de Boer², M. Busetta⁴, W.Collmar¹,
A. Connors³, R. Diehl¹, L. Hanlon⁴, J.W. den Herder², W. Hermsen²,
M. Kippen³, L. Kuiper², G. Lichti¹, J. Lockwood³, M. McConnell³, D. Morris³,
J. Ryan³, V. Schönfelder¹, G. Stacy³, H. Steinle¹, A.W. Strong¹,
B.N. Swanenburg², B.G. Taylor⁴, M. Varendorff¹, C.de Vries², O.R. Williams⁴

¹ Max-Planck Institut für extraterr. Physik, 8046 Garching, F.R.G.

² Laboratory for Space Research Leiden, 2300 RA Leiden, The Netherlands

³ University of New Hampshire, Durham, NH 03824, U.S.A.

⁴ Space Science Department of ESA, 2200 AG Noordwijk, The Netherlands

ABSTRACT

The imaging γ - ray telescope COMPTEL on board NASA's Compton Gamma - Ray Observatory (GRO) has observed many cosmic gamma-ray bursts during the early mission phase of GRO. COMPTEL records time-resolved burst spectra over 0.1 MeV to 10 MeV energies, and, for the first time, produces direct single-telescope gamma-ray images (0.8 MeV - 30 MeV) of cosmic gamma-ray bursts occurring in its 1 sr field of view.

INSTRUMENT AND OPERATING MODES

The imaging Compton telescope COMPTEL¹ is one of four instruments on board the Compton Gamma-Ray Observatory satellite (GRO), launched on space shuttle Atlantis on April 5, 1991 into a 450 km, 28.5° orbit. Gamma-ray bursts can be observed by COMPTEL using two independent operating modes, the "Double Scatter Mode" and the "Single Detector Mode". In the "Double Scatter Mode", which is the normal imaging mode, COMPTEL operates in the 0.8 MeV to 30 MeV range with a field of view of 1 steradian, an angular resolution of apx. 1° (1 σ), and an energy resolution of better than 10% FWHM. A gamma-ray photon is first Compton scattered in one of the 7 upper low-Z material detectors (D1 array, liquid scintillator NE 213A, total area 4188 cm²) followed by an interaction in a high-Z detector of the lower array (D2 array, 14 NaI cells, total area 8620 cm², see Figure 1). The measured quantities per event include the locations and energy deposits of these interactions in D1 and D2, the pulse shape of the interaction in the upper (D1) detector, the absolute time (125 μ s accuracy) of the event and the time-of-flight of the scattered photon from upper to lower detector.

Measurement of the pulse shape in D1 allows rejection of neutrons, and a suitable window set on the time-of-flight permits rejection of most of the background events (e.g. first scattered in D2 followed by an interaction in D1). The possible arrival directions for completely absorbed gamma events lie on a circle with radius ϕ around the direction of the scattered gamma-ray:

$$\cos(\phi) = 1 - \frac{mc^2}{E_2} + \frac{mc^2}{(E_1 + E_2)} \quad (1)$$

where mc^2 is the electron rest energy and E_1 and E_2 are the energy deposits of the gamma-ray in the upper and lower detector respectively (Figure 1). The

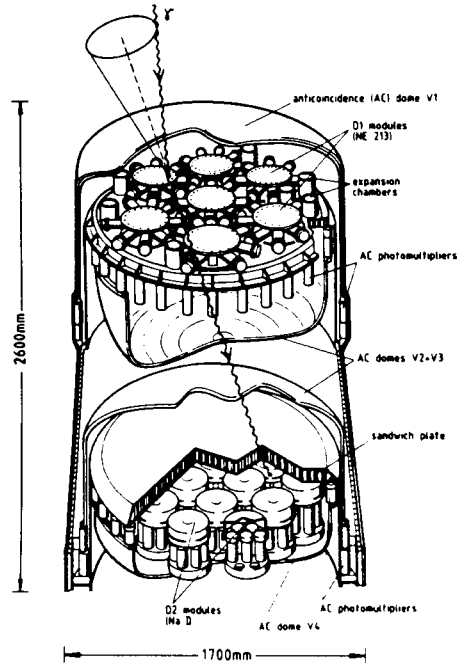


Figure 1. Schematic view of COMPTEL.

origin of emission can be located using event circles from different source gamma-rays. Events which are not completely absorbed in the NaI detector produce circles with too large radii, not intersecting at the source position. The "Single Detector Mode" is described in detail elsewhere². Summarising, COMPTEL uses 2 of the lower 14 NaI detectors (see Figure 1) to accumulate burst spectra upon receipt of a trigger signal from the Burst And Transient Source Experiment BATSE on board GRO. The detectors are, in principle, 4π sensitive. However, their on-axis field of view is largely obstructed by the upper D1 detector array. At larger zenith angles ($> 45^\circ$), obstruction is due to other GRO instruments, electronics boxes, spacecraft structure etc. The two detectors measure different energy regions: low range (apx. 0.1 MeV - 1.1 MeV, binwidth ~ 9.8 keV) and high range (apx. 1 MeV - 10 MeV, binwidth ~ 84.7 keV). In the absence of the BATSE trigger, background spectra (2 - 512 s telecommandable integration time) are accumulated and read out from both burst detectors. These data are used to investigate the total (instrumental + astrophysical) background before and after a burst event. After receipt of the BATSE burst trigger, 6 high resolution burst spectra (0.1 s to 25.6 s telecommandable integration time) are recorded. After the 6th spectrum a sequence of intermediate time resolution (tail) spectra (2 - 512 s telecommandable integration time) is accumulated and read out. After the last tail spectrum (maximum number = 255), the normal background mode is entered again. The configuration for the burst detector system during the initial mission phase was: background mode 100 s integration (consecutive integration and read-out); six burst spectra each with 0.5 s integration time; 133 tail spectra, each with 6 s integration time. The status of COMPTEL, at the time of this workshop, is as follows: After the termination of the tuning phase, the verification phase began on April 28, 1991, followed by the

24 COMPTEL Observations of Cosmic Gamma-Ray Bursts

nominal Phase I sky survey. While awaiting outgassing, detector modules D1-4 (switched off since July 1991) and D2-14 (the low range burst detector, switched off since 25 May 1991) are not operational for the time being. During the observation of GRB 910503 the modules D1-7, D2-1 and D2-5 were not operational.

SUMMARY OF GAMMA-RAY BURST OBSERVATIONS

During the period 21 April 1991 until 07 October 1991, COMPTEL received in total 729 trigger messages from BATSE identifying 138 cosmic gamma-ray bursts, 197 solar flares, 326 particle events, 49 triggers on SAA entry/exit and 19 others. Out of the 138 cosmic gamma-ray bursts, eleven events occurred inside or close to the COMPTEL field-of-view and they are therefore candidate objects for direct imaging and spectral analysis: These include GRB 910425 (onset: 2268 s UT); GRB 910503 (25455 s UT); GRB 910601 (69736 s UT); GRB 910609 (2909 s UT); GRB 910627 (16159 s UT); GRB 910714 (74779 s UT) and GRB 910814 (69275 s UT). The remaining events GRB 910711 (34314 s UT); GRB 910818 (49487 s UT) and GRB 911002 (31973 s UT) were too soft/weak to be detected in the telescope event data and during a short time interval including GRB 910927 (84414 s UT), COMPTEL was, unfortunately, switched off. The other 127 GRB's (outside the FOV) have been recorded by the single burst detectors for spectral analysis.

INDIVIDUAL RESULTS: GRB 910503

We present first results from GRB 910503. Further preliminary results on the other bursts listed above can be found elsewhere³ in these proceedings.

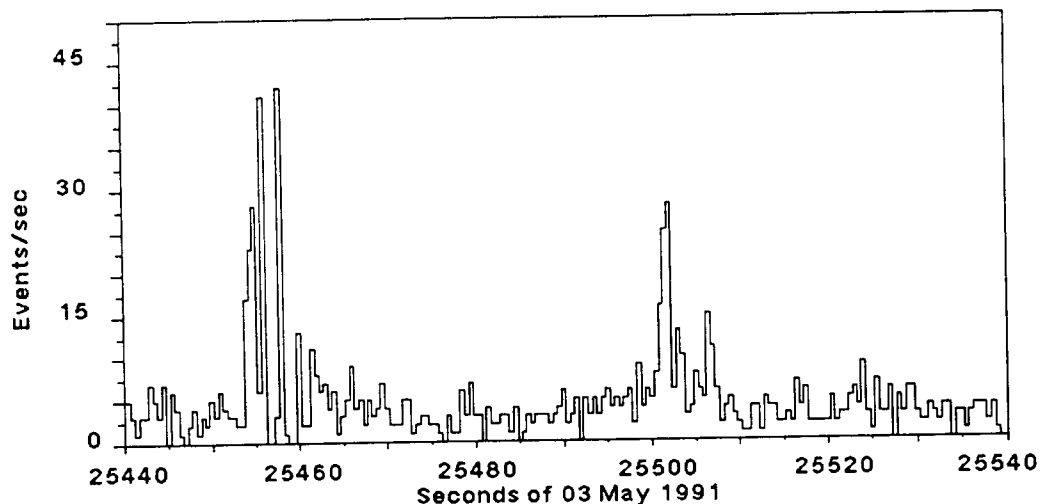


Figure 2. GRB 910503: Lightcurve from COMPTEL imaging events. Data contain raw events without application of any selection criteria.

The time history from “double scatter” events (Figure 2) clearly demonstrates that GRB 910503 was very bright compared to the typical event rate (~ 6 Hz), leading to a saturation of the event data buffers prior to data transmission. This explains the data gaps during the first (10 s) pulse. Inspection of the lightcurves obtained from the single burst detectors (Figure 3) shows that GRB

910503 consists of a main pulse with sub-second structure followed by a second small pulse 45 s after burst onset. The total duration of the burst is ~ 60 s. Figure 3 indicates significant differences in the shapes of the lightcurves of these two pulses. We have calculated hardness ratios by dividing the (background subtracted) time integrated count rate in the high range by the corresponding count rate of the low range detector. Both pulses including the two sub-pulses of the first pulse show a significant hard-to-soft evolution during the burst event (Figure 3). This is similar to earlier SMM results⁴ which showed that a hard-to-soft evolution is characteristic of bursts with pulses of ≥ 1 s duration.

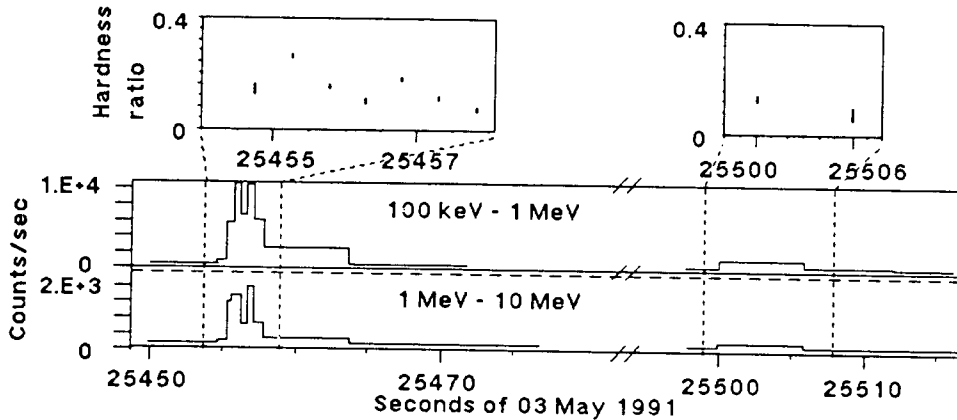


Figure 3. Lightcurves obtained from the COMPTEL burst detectors and hardness ratio for both pulses of GRB 910503.

The energy spectrum for each pulse as derived from telescope events is shown in Figure 4. GRB 910503 is a hard event with significant emission up to ~ 10 MeV. The best fit was achieved by fitting the count spectrum to a power-law folded through the simulated instrument response. Selecting 10 s of observed events from each pulse, using standard time-of-flight and pulse shape event selection windows and accepting all events from within $\pm 15^\circ$ around the burst position, we obtained the following power-law indices for best fit photon spectra: first pulse: $\alpha = -1.97 \pm 0.44(1\sigma)$, second pulse: $\alpha = -1.99 \pm 0.49(1\sigma)$.

The energy loss spectrum obtained from the single burst detectors is shown in Figure 5. Spectra obtained during the first pulse have been added and background subtracted. The count spectrum in each range was compared with a simulated count spectrum produced by a model power-law photon spectrum injected at the burst incidence direction into the COMPTEL mass model. Various power-law spectra in the range $E^{-1.7}$ to $E^{-2.3}$ were tested. Good agreement was obtained, again, for a $E^{-2.0}$ input spectrum averaged over the pulse consistent with the results from the telescope event spectrum. A thermal Bremsstrahlung law does not fit the observation. Our results indicate the presence of a non-thermal particle distribution at the source.

From energy integrated single detector count rates obtained during both pulses (Figure 3) we estimate the burst fluence to be $S(> 0.1\text{MeV}) \sim 2 \times 10^{-4} \text{ erg/cm}^2$ and $S(> 1.0\text{MeV}) \sim 7 \times 10^{-5} \text{ erg/cm}^2$. This is in good agreement with the fluence estimate derived from the telescope event photon spectrum (Figure 4) which gives $S(> 0.8\text{MeV}) = (8.6 \pm 1.5) \times 10^{-5} \text{ erg/cm}^2$. In order to accurately map the sky region around GRB 910503, we have used independent

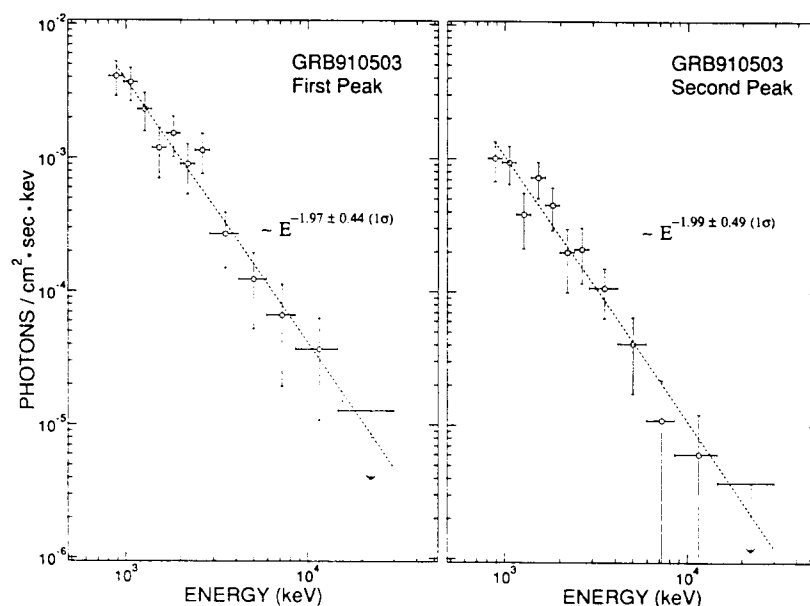


Figure 4. Best fit telescope event spectra for first pulse (25454 s - 25464 s) and second pulse (25500 s - 25510 s) of GRB 910503.

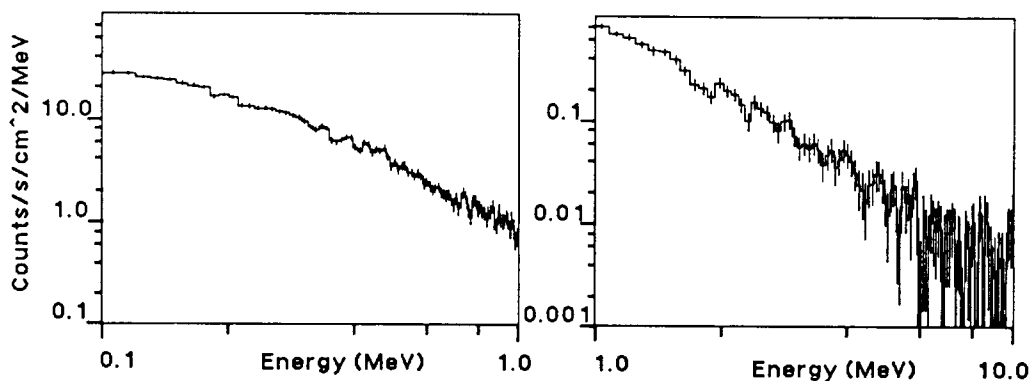


Figure 5. GRB 910503, first pulse: background subtracted spectra from both single detectors.

image restoration methods. The results of the maximum entropy method³ applied to GRB 910503 are shown in Figure 6. We have selected 193 candidate source events (1 -20 MeV) obtained between 25453 s and 25510 s (both pulses, Figure 2). The number of background events during 57 s is estimated to be about 30. Using event arrival time analysis with Ulysses data, we construct a triangulation circle which intersects at the position obtained by direct imaging (Figure 6).

The most likely position with its corresponding errors is determined using the maximum likelihood method resulting in a burst position of $(l,b) = (171.8^\circ, 6.4^\circ)$ with a 99% (2.6σ) statistical confidence radius of about 2° . The result is slightly dependent on the applied data selections. Due to the fact that this burst, being 31° off the telescope line-of-sight, is located near the edge of the COMPTEL field-of-view, a systematic error of up to 1° can not be excluded.

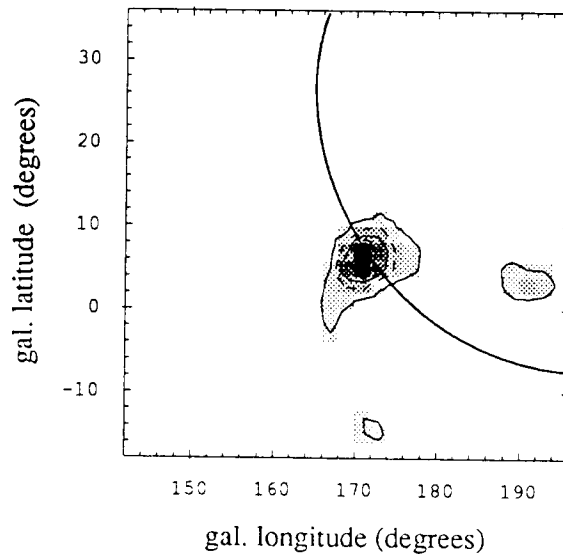


Figure 6. Maximum entropy skymap of the GRB 910503 burst region. The contours are given in relative flux units. The triangulation circle derived from COMPTEL/Ulysses arrival time analysis is shown.

CONCLUSIONS

It has been demonstrated that COMPTEL, the first imaging Compton telescope operational in space, has unique imaging capabilities in the largely unexplored 1 - 30 MeV energy band. The cosmic gamma-ray burst GRB 910503, so far the strongest of the bursts observed by COMPTEL in its field of view, is a "classical" hard transient, located near the galactic anticentre direction with significant emission up to several MeV. *For the first time a direct MeV image of a cosmic gamma-ray burst has been obtained.* Independent spectral data demonstrate that spectral evolution has been detected during both pulses indicating a softening of the non-thermal particle energy distribution on time scales of a few seconds.

REFERENCES

1. V. Schönfelder et al., IEEE Trans. Nucl. Sci. **31**, 766 (1984).
2. C. Winkler et al., Adv. Space Res. **6**, 113 (1986).
3. M. Varendorff et al., these proceedings, (1991).
4. J. Norris et al., Ap. J. **301**, 213 (1986).